Inorg. Chem. **2003**, *42*, 1296–1305

Chalcogenide-Halides of Niobium (V). 1. Gas-Phase Structures of $NbOBr_3$, $NbSBr_3$, and $NbSCl_3$. 2. Matrix Infrared Spectra and Vibrational Force Fields of $NbOBr_3$, $NbSBr_3$, $NbSCl_3$, and $NbOCl_3$

Izabela Nowak,[†] Elizabeth M. Page,[‡] David A. Rice,*[,‡] Alan D. Richardson,[§] Richard J. French,[§] Kenneth Hedberg,*[,§] and J. Steven Ogden[||]

Department of Chemistry, University of Reading, Whiteknights, Reading RG6 6AD, U.K., Department of Chemistry, Oregon State University, Corvallis, Oregon 97331, and Department of Chemistry, University of Southampton, Highfield Road, Southampton SO17 1BJ, U.K.

Received June 17, 2002

The molecular structures of $NbOBr_3$, $NbSCl_3$, and $NbSBr_3$ have been determined by gas-phase electron diffraction (GED) at nozzle-tip temperatures of 250 °C, taking into account the possible presence of $NbOCl_3$ as a contaminant in the $NbSCl_3$ sample and $NbOBr_3$ in the $NbSBr_3$ sample. The experimental data are consistent with trigonal-pyramidal molecules having C_{3v} symmetry. Infrared spectra of molecules trapped in argon or nitrogen matrices were recorded and exhibit the characteristic fundamental stretching modes for C_{3v} species. Well resolved isotopic fine structure (^{35}Cl and ^{37}Cl) was observed for $NbSCl_3$, and for $NbOCl_3$ which occurred as an impurity in the $NbSCl_3$ spectra. Quantum mechanical calculations of the structures and vibrational frequencies of the four $YNbX_3$ molecules (Y = O, S; X = Cl, Br) were carried out at several levels of theory, most importantly B3LYP DFT with either the Stuttgart RSC ECP or Hay–Wadt ($n + 1$) ECP VDZ basis set for Nb and the 6-311G* basis set for the nonmetal atoms. Theoretical values for the bond lengths are 0.01–0.04 Å longer than the experimental ones of type r_a, in accord with general experience, but the bond angles with theoretical minus experimental differences of only 1.0–1.5° are notably accurate. Symmetrized force fields were also calculated. The experimental bond lengths (r_g/Å) and angles ($\angle_\alpha$/deg) with estimated 2σ uncertainties from GED are as follows. $NbOBr_3$: r(Nb═O) = 1.694(7), r(Nb—Br) = 2.429(2), ∠(O═Nb—Br) = 107.3(5), ∠(Br—Nb—Br) = 111.5(5). $NbSBr_3$: r(Nb═S) = 2.134(10), r(Nb—Br) = 2.408(4), ∠(S═Nb—Br) = 106.6(7), ∠(Br—Nb—Br) = 112.2(6). $NbSCl_3$: r(Nb═S) = 2.120(10), r(Nb—Cl) = 2.271(6), ∠(S═Nb—Cl) = 107.8(12), ∠(Cl—Nb—Cl) = 111.1(11).

Introduction

Our structural interest in the compounds of this investigation began over 25 years ago when we developed room-temperature synthetic routes to the materials $NbSCl_3$ and $NbSBr_3$.[1] These ternary compounds presented a structural challenge because attempts to obtain crystals by sublimation led to complex reactions indicated by color changes that occurred on heating the materials in sealed tubes under vacuum. Having successfully used the GED method to determine the molecular structures of the tungsten(VI) chalcogeno-chlorides $WSCl_4$ and $WSeCl_4$,[2] and the related bromides $WOBr_4$,[3] $WSeBr_4$,[4] and $WSBr_4$,[4] a similar application of the method to the niobium(V) chalcogeno-halides was clearly indicated. We expected the study of these compounds to be more challenging than those of the tungsten compounds, and it turned out to be so. An initial report of GED work on $NbOBr_3$ and $NbSBr_3$ is given in the thesis of R. J. French.[5] We have now extended the original work to include matrix-

* Authors to whom correspondence should be addressed. E-mail: hedbergk@chem.ucs.orst.edu (K.H.); dia.rice@reading.ac.uk. (D.A.R.).
[†] Present address: Faculty of Chemistry, A. Mickiewicz University, Grunwaldzka 6, 60-780 Poznan, Poland.
[‡] University of Reading.
[§] Oregon State University.
[||] University of Southampton.

(1) Fowles, G. W. A.; Hobson, R. J.; Rice, D. A.; Shanton, K. J. *J. Chem. Soc.* **1976**, 55.
(2) Page, E. M.; Rice, D. A.; Hagen, K.; Hedberg, L.; Hedberg, K. *Inorg. Chem.* **1982**, *21*, 3280.
(3) Page, E. M.; Rice, D. A.; Hagen, K.; Hedberg, L.; Hedberg, K. *Inorg. Chem.* **1987**, *26*, 467. See also: Shishkin, N. Ya.; Zharsky, I. M.; Novikov, G. I. *J. Mol. Struct.* **1981**, *73*, 249.
(4) Page, E. M.; Rice, D. A.; Hagen, K.; Hedberg, L.; Hedberg, K. *Inorg. Chem.* **1991**, *30*, 4758.
(5) French, R. J. Ph.D. Thesis, Oregon State University, 1987.

10.1021/ic020405f CCC: $25.00
Published on Web 01/24/2003

isolated infrared spectroscopic data on $NbSCl_3$ and $NbSBr_3$, and ab initio molecular orbital calculations on these compounds as well as on the corresponding oxygen homologues and on $NbCl_5$. Of interest in its own right, this spectroscopic and theoretical work was an important aid in the GED analyses.

In the years following French's thesis work, accounts of several GED studies of other niobium compounds ($NbOF_3$,[6] $NbOCl_3$[7] and $NbOI_3$,[8]) have appeared. The results for all the niobium compounds are consistent with C_{3v} symmetry for the molecules in the gas phase. The present work makes use of French's diffraction patterns for his compounds, and patterns for $NbSCl_3$ from new experiments. The main purpose of our studies of the title molecules was to identify the structural changes that occur with changes in the ligands and to account for these both here and in other $NbYX_3$ molecules in terms of the nature of the bonding and steric interactions. A satisfactory understanding of these effects in the WYX_4 compounds (Y, a group 16 element; X, a group 17 element) was obtained through the work already cited, and by additional investigations of WOF_4,[9] $WOCl_4$,[10] WSF_4,[11] and $WSeF_4$.[12]

Experimental Section

Preparation of Compounds. Details of the synthetic methods for creating a range of oxo- and sulfido-trihalides have been previously published in several articles.[1,13] A brief description of the relevant material is presented here. Because the isolated compounds are very air and moisture sensitive, preparation and purification were carried out using an all-glass vacuum line. Care was taken to remove surface moisture from the vacuum line and sample ampules by heating the glassware under a high and dynamic vacuum to approximately 100 °C for 3 h. The vacuum line and glovebox were filled with dry, oxygen-free nitrogen when solid products were transferred to sample ampules or while preparing compounds for analysis.

The chalcogenide trihalides, golden yellow $NbSCl_3$ and red-orange $NbSBr_3$, were prepared by allowing NbX_5 (X = Cl or Br) to react with Sb_2S_3 at a 3:1 molar ratio in carbon disulfide at room temperature:

$$3NbX_5 + Sb_2S_3 \rightarrow 3NbSX_3 + 2SbCl_3$$

The niobium halides were prepared by the halogenation of metal sheet at 300 °C (X = Cl) and 350 °C (X = Br). Prior to their use, the halogens (chlorine and bromine) were dried using concentrated sulfuric acid and P_2O_5. High surface area Sb_2S_3 was prepared by passing H_2S through acidified aqueous solutions of $SbCl_3$. The reaction medium, CS_2, was dried over P_2O_5 and distilled three times onto fresh P_2O_5 before use.

Preparation of the sulfido-halides began by placing about 5 g of the corresponding niobium halide into a previously weighed reaction ampule containing a Teflon-coated magnetic stirrer. The ampule was quickly evacuated and left under a dynamic vacuum for 0.5 h. At the end of this time, the ampule was reweighed. A cooled sample of Sb_2S_3, previously held under a dynamic vacuum for 12 h at 200 °C, was added to the ampule in an amount sufficient to give a halide-to-sulfide ratio slightly greater than 3:1. The ampule was then evacuated, cooled to −196 °C, filled with CS_2, sealed, and allowed to warm to room temperature, at which point the mixture was stirred for 24 h. Extending the reaction time for the chloride beyond 24 h led to the formation of some $Nb_2S_3Cl_4$, and it is the formation of this darker material that we believe has led to the variety of colors ascribed to $NbSCl_3$ in the literature.[14,15] The insoluble sulfido-halides were isolated by vacuum filtration. The product was washed with copious amounts of dry CS_2 to remove any occluded $SbCl_3$. Finally, the product was subjected to a dynamic vacuum for 24 h.

The oxo-halide $NbOBr_3$ was prepared in a manner similar to that for $NbSBr_3$ except that resublimed commercial Sb_2O_3 was used instead of Sb_2S_3. The purity of the sulfido- and oxo-halides was confirmed[15] by determination of halide and niobium concentration using classical methods.

Matrix Isolation Infrared Spectroscopy. Extensive matrix isolation studies were carried out on samples of $NbSCl_3$ and $NbSBr_3$, which were vaporized from break-seal ampules in an all-glass system. Temperatures in the 90−110 °C range produced sufficient sample vapor which was cocondensed with a large excess ($> \times 1000$) of the matrix gas onto a CsI window cooled to 12 K. High purity nitrogen and argon (99.999%) were used as matrix materials. All infrared spectra were recorded on a Perkin-Elmer 983G spectrophotometer; the general features of the matrix isolation apparatus have been described elsewhere.[16]

In addition to obtaining matrix IR data on $NbSCl_3$ and $NbSBr_3$, these studies also yielded matrix IR spectra of $NbOCl_3$ and $NbOBr_3$ formed in small (and variable) amounts as a result of hydrolysis reactions arising from interaction with the glass surfaces. These molecules were identified by comparison with earlier studies, but in the case of $NbOCl_3$, it was possible to carry out a more detailed analysis of the vibrational spectrum than was currently available.

Theoretical Calculations. Geometry optimizations and frequency calculations of $NbOBr_3$, $NbSBr_3$, $NbSCl_3$, $NbOCl_3$, and $NbCl_5$ were carried out at the B3LYP DFT level of theory with use of the Gaussian 98W program.[17] ($NbOCl_3$, which occurs as a reaction byproduct, was found to be a likely impurity and $NbCl_5$ a possible one.) The basis sets included the Stuttgart RSC ECP or Hay−Wadt ($n + 1$) ECP VDZ bases for Nb and 6-311G* for Br, Cl, O, and S. The principal role of these calculations was to yield the basis, i.e. quadratic force fields, for interconversion of certain types of interatomic distances that figure in the structure analysis

(6) Belova, I. N.; Giricheva, N. I.; Girichev, G. V.; Shlykov, S. A. *J. Struct. Chem.* **1997**, *37*, 609.
(7) Belova, I. N.; Giricheva, N. I.; Grichev, G. V.; Petrova, V. N.; Shlykov, S. A. *J. Struct. Chem.* **1996**, *37*, 224.
(8) Giricheva, N. I.; Girichev, G. V.; Shylokov, S. A.; Pavlova, G. Yu.; Sysoev, S. V.; Golubenko, A. N.; Titov, V. A. *J. Struct. Chem.* **1993**, *33*, 517.
(9) Robiette, A. G.; Hedberg, K.; Hedberg, L. *J. Mol. Struct.* **1977**, *37*, 105.
(10) (a) Spiridonov, V. P.; Zasorin, E. Z.; Zharskii, I. M.; Novikov, G. I. *J. Struct. Chem.* **1972**, *13*, 511. (b) Iijima, K.; Shibata, S. *Bull. Chem. Soc. Jpn.* **1974**, *47*, 1393. (c) Zharskii, J. M.; Novikov, G. I.; Zasorin, E. Z.; Spiridonov, P., IV. *Dokl. Akad. Nauk. BSSR* **1976**, *20*, 234.
(11) Rice, D. A.; Hagen, K,; Hedberg, L.; Hedberg, K.; Staunton, G. M.; Holloway, J. H. *Inorg. Chem.* **1984**, *23*, 1826.
(12) Hagen, K.; Rice, D. A.; Holloway, J. H.; Kaučič, V. *J. Chem. Soc., Dalton Trans.* **1986**, 1821.
(13) (a) Fowles, G. W. A.; Hobson, R. J.; Rice D. A.; Shanton K. J. *J. Chem. Soc., Chem. Commun.* **1976**, 552. (b) Drew, M. G. B.; Rice, D. A.; Williams, D. M. *J. Chem. Soc., Dalton Trans.* **1983**, 2251. (c) Drew, M. G. B.; Rice, D. A.; Williams, D. M. *J. Chem. Soc., Dalton Trans* **1985**, 417. (d) Sands, D. E.; Zalkin, A.; Elson, R. E. *Acta Crystallogr.* **1959**, *12*, 21. (e) Drew, M. G. B.; Tomkins, I. B. *Acta Crystallogr., Sect. B* **1970**, *26*, 1161.
(14) Fairbrother, F.; Cowley, A. H.; Scott, N *J. Less-Common Met.* **1959**, *1*, 206.
(15) Baba, I. B. PhD thesis, University of Reading, 1977.
(16) Ogden, J. S.; Wyatt, R. S. *J. Chem. Soc., Dalton Trans.* **1987**, 859.

Table 1. Theoretical Symmetry Force Constants and Wavenumbers/cm^{-1} for $NbYX_3$ Molecules[a,b]

		$NbOCl_3$				$NbOBr_3$				
		$F_{1(4)}$	$F_{2(5)}$	$F_{3(6)}$	ω	$F_{1(4)}$	$F_{2(5)}$	$F_{3(6)}$	ω	mode
a_1	F_1	7.914			993	7.931			994	Nb═Y str
		8.108			*1005*	*8.020*			*1000*	
	F_2	0.408	3.026		401	0.349	2.418		252	Nb−X str
		0.398	*2.821*		*388*	*0.350*	*2.399*		*252*	
	F_3	−0.150	0.051	0.536	127	−0.148	0.031	0.552	96	Y═Nb−X bend
		−0.154	*0.050*	*0.550*	*128*	*−0.148*	*0.030*	*0.544*	*96*	
e	F_4	2.564			447	2.196			342	Nb−X str
		2.413			*436*	*2.066*			*334*	
	F_5	−0.070	0.686		222	−0.049	0.671		197	Y═Nb−X bend
		−0.069	*0.710*		*222*	*−0.047*	*0.680*		*197*	
	F_6	0.067	−0.025	0.350	101	0.045	−0.025	0.369	68	X−Nb−X bend
		0.065	*−0.026*	*0.342*	*101*	*0.043*	*−0.025*	*0.369*	*68*	

		$NbSCl_3$				$NbSBr_3$				
		$F_{1(4)}$	$F_{2(5)}$	$F_{3(6)}$	ω	$F_{1(4)}$	$F_{2(5)}$	$F_{3(6)}$	ω	mode
a_1	F_1	4.397			565	4.355			561	Nb═Y str
		4.573			*576*	*4.505*			*570*	
	F_2	0.291	2.956		395	0.256	2.403		250	N−X str
		0.288	*2.787*		*384*	*0.259*	*2.384*		*250*	
	F_3	−0.083	0.078	0.561	128	−0.080	0.060	0.589	96	Y═Nb−X bend
		−0.086	*0.077*	*0.578*	*128*	*−0.081*	*0.060*	*0.579*	*96*	
e	F_4	2.536			440	2.193			330	Nb−X str
		2.412			*429*	*2.069*			*322*	
	F_5	−0.031	0.677		151	−0.008	0.684		129	Y═Nb−X bend
		−0.031	*0.698*		*150*	*−0.008*	*0.686*		*129*	
	F_6	0.062	−0.010	0.355	102	0.042	−0.011	0.385	69	X−Nb−X bend
		0.062	*−0.010*	*0.355*	*102*	*0.041*	*−0.011*	*0.379*	*69*	

[a] Numbers in regular typeface are scaled force constants from B3LYP/Stuttgart theory with use of experimental wavenumbers when available; italicized numbers are from theory only. [b] Values are aJ/Å^2 for stretches, aJ/Å·rad for stretch−bends, and aJ/rad^2 for bends.

and for the calculation of amplitudes of vibration that could not be reliably measured; no direct use was made of the optimized geometries. The Cartesian force fields from the Stuttgart calculations were converted to symmetrized force fields with the program ASYM40[18] and scaled in such a way as to provide a fit to available experimental wavenumbers ($NbOBr_3$,[19,20a] $NbOCl_3$,[21] $NbSBr_3$,[20a] $NbSCl_3$[20b]). Theoretical vibrational wavenumbers from the B3LYP/Stuttgart calculations were used when experimental ones were unavailable. The symmetry force constants from this procedure were used to calculate corrections for the effects of vibrational averaging. Table 1 contains the two sets of symmetrized force constants. and Table 2 gives the symmetry coordinates used for this work. Similar calculations were also done for $NbCl_5$,[22] but results for this molecule did not figure importantly in the analyses and the results have not been tabulated.

Table 2. Symmetry Coordinates for $NbYX_3$ Molecules[a]

a_1	$S_1 = \Delta r_{12}$	Nb═Y str
	$S_2 = 1/\sqrt{3}\Delta(r_{13} + r_{14} + r_{15})$	Nb−X str
	$S_3 = 1/\sqrt{6}\Delta(\alpha_{213} + \alpha_{214} + \alpha_{215} - \beta_{314} - \beta_{415} - \beta_{513})$	Y═Nb−X bend
e	$S_4 = 1/\sqrt{6}\Delta(2r_{13} - r_{14} - r_{15})$	Nb−X str
	$S_5 = 1/\sqrt{6}\Delta(2\alpha_{213} - \alpha_{214} - \alpha_{215})$	Y═Nb−X bend
	$S_6 = 1/\sqrt{6}\Delta(2\beta_{314} - \beta_{415} - \beta_{513})$	X−Nb−X bend
	$S_7 = 1/\sqrt{2}\Delta(r_{13} - r_{14})$	Nb−X str
	$S_8 = 1/\sqrt{2}\Delta(\alpha_{214} - \alpha_{215})$	Y═Nb−X bend
	$S_8 = 1/\sqrt{2}\Delta(\beta_{415} - \beta_{513})$	X−Nb−X bend

[a] Atom numbering: 1 = Nb; 2 = Y; 3, 4, 5 = X.

Electron Diffraction. GED measurements were carried out using the apparatus at Oregon State University. Samples of the niobium compounds ($NbOBr_3$, $NbSCl_3$, and $NbSBr_3$) were held in sealed, 30 cm long glass ampules equipped with break-seals and were attached as needed to the apparatus with the use of a 1/4 in. Swagelock fitting. With the ampules under vacuum, the tubing above the break-seals was heated to at least 120 °C for 1 h to remove occluded moisture. The ampule was opened by dropping a small, glass-encased metal plug onto the break-seal, and the sample tube was then wrapped with heating tape and gradually warmed. Vapor sufficient to produce good photographs was obtained with bulk sample temperatures of about 250 °C. The nozzle inlet tube was heated to a slightly higher temperature to prevent condensation. Photographs were recorded on Kodak projector slide plates (medium contrast) and were developed in D-19 diluted 1 to 1. The best photographs from each experiment were chosen for analysis. The diffraction photographs for $NbOBr_3$ and $NbSBr_3$ were those made for French's thesis work but analyzed afresh with our improved procedures in order to be consistent with those applied to the new experiments on $NbSCl_3$. Each plate was traced and digitized with

(17) Frisch, M. J.; Trucks, G. W.; Schlegel, H. B.; Scuseria, G. E.; Robb, M. A.; Cheeseman, J. R.; Zakrzewski, V. G.; Montgomery, J. A., Jr.; Stratmann, R. E.; Burant, J. C.; Dapprich, S.; Millam, J. M.; Daniels, A. D.; Kudin, K. N.; Strain, M. C.; Farkas, O.; Tomasi, J.; Barone, V.; Cossi, M.; Cammi, R.; Mennucci, B.; Pomelli, C.; Adamo, C.; Clifford, S.; Ochterski, J.; Petersson, G. A.; Ayala, P. Y.; Cui, Q.; Morokuma, K.; Malick, D. K.; Rabuck, A. D.; Raghavachari, K.; Foresman, J. B.; Cioslowski, J.; Ortiz, J. V.; Baboul, A. G.; Stefanov, B. B.; Liu, G.; Liashenko, A.; Piskorz, P.; Komaromi, I.; Gomperts, R.; Martin, R. L.; Fox, D. J.; Keith, T.; Al-Laham, M. A.; Peng, C. Y.; Nanayakkara, A.; Gonzalez, C.; Challacombe, M.; Gill, P. M. W.; Johnson, B.; Chen, W.; Wong, M. W.; Andres, J. L.; Gonzalez, C.; Head-Gordon, M.; Replogle, E. S.; Pople, J. A. *Gaussian 98*, revision A.7; Gaussian, Inc.: Pittsburgh, PA, 1998.
(18) Hedberg, L.; Mills, I. M. *J. Mol. Spectrosc.* **2000**, *203*, 82.
(19) Schulz, C. O.; Stafford, F. E. *J. Phys. Chem*. **1968**, *72*, 4686.
(20) (a) This work. (b) Nowak, I. MSc. Thesis, University of Reading, 1993.
(21) (a) Beattie, I. R.: Livingstone, K. M. S.; Reynolds, D. J.; Ozin, G. A. *J. Chem. Soc. A* **1970**, 1210. (b) Ozin, G. A.; Reynolds, D. J. *J. Chem. Soc., Chem. Commun.* **1969**, 884.
(22) (a) Beattie, I. R.; Ozin, G. A. *J. Chem. Soc. A* **1969**, 1691. (b) Ischenko, A. A.; Strand, T. G.; Demidov A. V.; Spiridonov, V. P. *J. Mol. Struct.* **1978**, *43*. 227. (c) Zavalishin, N.; Cand. Diss., University of Moscow, 1975.

Table 3. Experimental Conditions for $NbOBr_3$, $NbSBr_3$, and $NbSCl_3$

	$NbOBr_3$		$NbSBr_3$	$NbSCl_3$	
	LC	MC	MC	LC	MC
sample temperature, °C	331	299	260	250	248
nozzle temperature, °C	352	307	268	310	307
ambient pressure/Torr × 10^{-6}	1.7−1.8	1.5−1.8	4.0−4.4	1.4	3.8−6.0
acceleration voltage/kV	45	48	48	60	60
beam currents/μA	0.41−0.44	0.43−0.52	0.46−0.47	0.30	0.45
exposure times/s	75−100	180−300	105−240	120−180	150−255
nominal electron wavelength/Å	0.0566	0.0549	0.0549	0.0484	0.0483
nozzle-to-plate distance/mm	744.29	300.42	300.58	746.78	298.46
no. of plates	4	5	4	2	2
traces per plate	1	1	3	3	3
data range, s_{min}/Å^{-1} to s_{max}/Å^{-1} [a]	2.00−12.75	6.00−32.00	4.50−32.25	2.00−16.50	7.00−30.00
data interval/Å^{-1} [a]	0.25	0.25	0.25	0.25	0.25
calibration substance	CO_2	CO_2	CO_2	CS_2	CS_2
r_a(C═S)/Å, or r_a(C═O)/Å	1.1646	1.1646	1.1646	1.557	1.557
r_a(S···S)/Å, or r_a(O···O)/Å	2.3244	2.3244	2.3244	3.109	3.109

[a] $s = 4\pi\lambda^{-1}\sin(\theta/2)$.

a modified Joyce-Lobel microdensitometer. In most cases, a plate was traced three times, and the resulting curves were averaged. The experimental conditions employed for each sample are listed in Table 3. The scattered intensities are available as Supporting Information.

Results

Matrix Isolation Infrared Spectroscopy. Matrix isolation spectroscopy provided a convenient method to investigate the vapor generated from heated $NbSX_3$ (X = Cl or Br) samples. The infrared spectra of $NbSCl_3$ and $NbSBr_3$ in argon and nitrogen matrices contain prominent bands in the Nb═S and Nb−X stretching regions. Some impurities were noticeable in the initial matrix deposits; the most obvious were $SbCl_3$, a synthesis product, and the oxo-halides $NbOCl_3$ and $NbOBr_3$. The latter two are believed to have been formed by the hydrolysis of the sulfido-halides as they passed through parts of the glass inlet system which could not be adequately heated to remove adsorbed water. The identity of the impurities was established by comparison with previous work.[23] The presence of the oxo-halides could be readily detected by their characteristic Nb═O vibrations at 990 cm^{-1}, and these higher wavenumber features did not present any problems regarding spectral interpretation. In the Nb−Cl and Nb−Br stretching regions, however, the presence of these impurities was found to complicate band assignments for both $NbSCl_3$ and $NbSBr_3$. A concern prior to the experiment was that heating the samples would form the species NbX_5 and $Nb_2S_3X_4$ and that only the former would be a volatile product, but there was no evidence of NbX_5 in the matrix.

Figure 1 shows typical low-resolution (5 cm^{-1}) matrix infrared spectra for deposits of $NbSBr_3$ (a and b) in a nitrogen matrix, and $NbSCl_3$ (c) in an argon matrix. The prominent bands at 560.9 (Nb═S) and 329.6 cm^{-1} (Nb−Br) in Figure 1a,b are assigned to $NbSBr_3$. In Figure 1a, the peak at 987.9 cm^{-1} (Nb═O) and the shoulder at 341.3 cm^{-1} (Nb−Br) are assigned to the impurity $NbOBr_3$. Both of these absorptions are much less prominent in Figure 1b, leading to the conclusion that this deposit contains less of the impurity. Although a third, weaker, feature is expected for $NbSBr_3$ at lower wavenumber, no such peak was found in the 330−200 cm^{-1} range in any of the spectra. The possibility remains that it lies too close to the 330 cm^{-1} band to be observed independently. To prevent buildup of the $NbOCl_3$ impurity in the $NbSCl_3$ deposition, the apparatus was "seasoned" prior to use by flowing $NbSCl_3$ vapor through the system. In Figure 1c, there is no discernible feature in the Nb═O stretching region, and the three bands at 565, 439, and 393 cm^{-1} are assigned as $NbSCl_3$ fundamentals. Table 4 lists band positions from this and previous work, and assignments for four $NbYX_3$ molecules. A comparison of the listings in the table shows that in the Nb═S stretching region both matrix hosts give essentially the same vibration frequencies at low resolution.

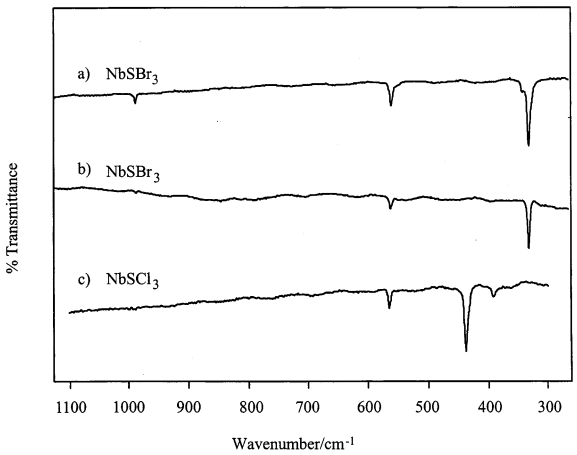

Figure 1. Low-resolution matrix isolation infrared spectra for $NbSBr_3$ and $NbSCl_3$. Spectra for $NbSBr_3$ (a and b) are from molecules isolated in a nitrogen matrix and show different amounts of $NbOBr_3$ impurity. Spectrum (c) shows $NbSCl_3$ in an argon matrix.

High-resolution spectra of the Nb−Cl stretching region are displayed in Figure 2. The uppermost experimental curve in Figure 2 is from a matrix deposit containing very little of the $NbOCl_3$ impurity. The well-resolved structure arises from the presence of chlorine isotopes ^{35}Cl and ^{37}Cl in natural abundance. The observed structure is highly diagnostic[24] of a C_{3v} trichloride unit, and the patterns at 440 and 390 cm^{-1}

(23) Nunziante-Cesaro, S.; Maltese, M.; Spoliti, M.; Janis, B. *Spectrochim. Acta, Part A* **1984**, *40*, 579.

Table 4. Theoretical and Experimental Wavenumbers/cm^{-1} for Stretching Vibrations of $NbYX_3$ Molecules[a]

		Nb═Y, A_1			Nb−X, E			Nb−X, A_1		
species	matrix	theory	current	lit.	theory	current	lit.	theory	current	lit.
$NbOCl_3$	N_2		996/993	[997/993]		444	[443]			
	Ar		993	[993]		448	[449]		400	
	vapor	1005		{997}	436		{448}	388		{395}
$NbOBr_3$	N_2		987.9	[989]		341.3	[339]			
	Ar		985.0							
	vapor	1000		(994)	333			252		
$NbSCl_3$	N_2		563.2			437			390	
	Ar		565.0			439			393	
	vapor	576			429			384		
$NbSBr_3$	N_2		560.9			329.6			*b*	
	Ar		558.5			330.0			*b*	
	vapor	570			322			250		

[a] Values in square brackets are from ref 23, those in braces are from ref 21a, and those in parentheses are from ref 19. [b] See text.

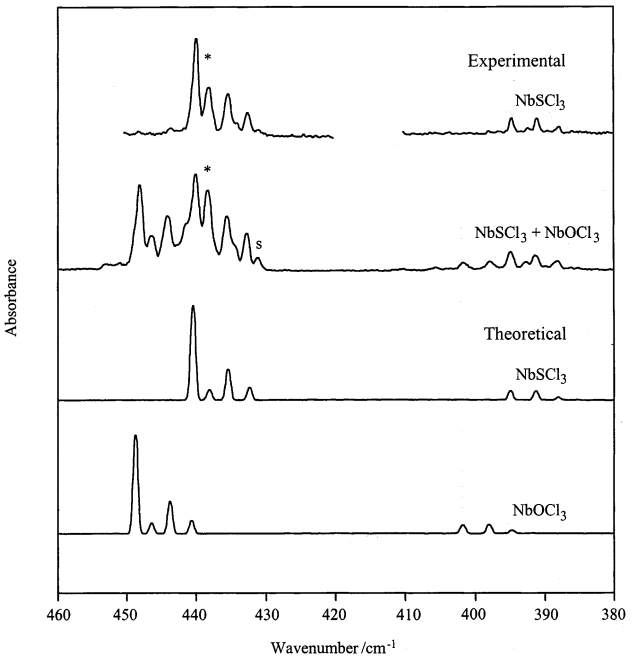

Figure 2. High-resolution infrared spectra from $NbSCl_3$ molecules isolated in an argon matrix. See text for full description.

are identified as arising from the E and A_1 Nb−Cl stretching modes. The other experimental curve is from a deposit containing both $NbSCl_3$ and $NbOCl_3$. The latter compound has not been studied at this level of detail,[23] but a comparison of the additional features observed in this spectrum to those above suggest their identification as isotopic structure arising from the analogous E and A_1 Nb−Cl modes in $NbOCl_3$. A listing of experimental and theoretical results for the various Nb−Cl isotopic components and their assignments can be found in Table 5.

The spectral assignments given in Tables 4 and 5 arise directly from a "stretching modes only" vibrational analysis on the C_{3v} monomers. The stretching modes in these $NbYX_3$ compounds have symmetries A_1 (Nb═Y), and $A_1 + E$ (Nb−X). A force field which suitably simulates the frequencies of the various isotopic species in the stretching region[24] contains two principal stretching force constants, $F_{(Nb=Y)}$ and $F_{(Nb-X)}$, and two stretch−stretch interaction constants. These four parameters, together with bond angles, permit the vibrational modeling of all isotopic components in the stretching region. Additionally, it has been shown that this model can successfully reproduce relative infrared band intensities, using the bond−dipole approach.[24] Theoretical spectra calculated for the niobium−chlorine region of $NbSCl_3$ and $NbOCl_3$ made use of the extensive isotopic data obtained by matrix isolation and assumed bond angles, respectively, of 107.0° and 106.7°.[25] These accompany the experimental spectra shown in Figure 2. The satisfactory agreement between the experimental and theoretical spectra forms the basis for the proposed band assignments listed in the tables. The enhanced intensity of the component at 437.9 cm^{-1}, denoted by "*", is believed to arise from a second site in the matrix which produces an equivalent, but displaced, isotope pattern. This also explains the additional weak feature in the figure observed at 430.8 cm^{-1} denoted by "s". (Bromine also has two naturally occurring isotopes, ^{79}Br and ^{81}Br, but the isotopic splitting associated with the Nb−Br

Table 5. Observed and Calculated Isotopic Wavenumbers/cm^{-1} for $NbOCl_3$ and $NbSCl_3$ in Argon Matrices

$NbOCl_3$		$NbSCl_3$		
obsd[a]	calcd[b]	obsd[a]	calcd[c]	assignment
993.0	993.0			A_1 Nb = O
		565.0	565.0	A_1 Nb = ^{32}S
		552.9	552.2	A_1 Nb = ^{34}S
447.8	448.3	439.7	440.0	E $Nb^{35}Cl_3$ + A″$Nb^{37}Cl^{35}Cl_2$
445.9	445.9	437.9	437.7	A′ $Nb^{35}Cl^{37}Cl_2$
443.6	443.2	435.2	435.1	A′ $Nb^{37}Cl^{35}Cl_2$
440.9	440.1	432.4	432.1	E $Nb^{37}Cl_3$ + A″$Nb^{35}Cl^{37}Cl_2$
		430.8		site effect, see text
401.5	401.6	395.0	395.0	A_1 $Nb^{35}Cl_3$
397.9	397.4	391.4	391.4	A′ $Nb^{37}Cl^{35}Cl_2$
	394.1	388.2	388.2	A′ $Nb^{35}Cl^{37}Cl_2$
	391.8		385.0	A_1 $Nb^{37}Cl_3$

[a] Argon matrix. [b] Based on a value of 107° for the angle O−Nb−Cl (ref 25) and assuming the following force constant values/mdyn·Å^{-1}: $F_{(Nb=O)} = 8.045$, $F_{(Nb-Cl)} = 2.869$, $F_{(Nb-Cl,Nb--Cl)} = 0.105$, $F_{(Nb=O,Nb-Cl)} = 0.6$. [c] Based on a value of 106.7° for the angle S−Nb−Cl (ref 25) and assuming the following force constant values/mdyn·Å^{-1}: $F_{(Nb=S)} = 4.584$, $F_{(Nb-Cl)} = 2.780$, $F_{(Nb-Cl,Nb-Cl)} = 0.147$, $F_{(Nb=S,Nb-Cl)} = 0.5$.

(24) (a)Wilson, E. B.; Decius, J. C.; Cross, P. C. *Molecular Vibrations*; McGraw-Hill: New York, 1955; p 166. (b) Beattie, I. R.; Blayden, H. E.; Hall, S. M.; Jenny, S. N.; Ogden, J. S. *J. Chem. Soc., Dalton Trans.* **1987**, 859.

(25) These angles were invoked before our results for $NbSCl_3$ were available. They are, however, close to the measured values for each compound (see ref 7 for $NbOCl_3$).

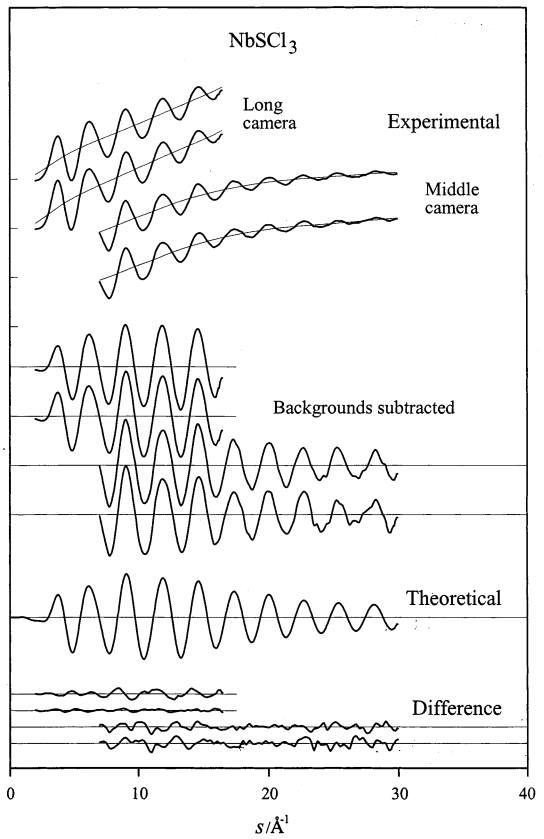

Figure 3. Intensity curves for $NbSCl_3$. Curves of the data from each exposure amplified five times are shown superimposed on their backgrounds; each is the average of three photometric traces. The background-subtracted curves are the molecular intensities on which the refinements were based. The difference curves are experimental minus theoretical for the final model (A). See Table 6 for model details.

stretching modes in $Nb{-}Br_3$ and $NbOBr_3$ is too small to be resolved with the apparatus available.)

The assignments given in Tables 4 and 5 are also supported from the purely quantum-mechanical side. For example, the wavenumbers calculated for the bond-stretching modes of $NbOCl_3$ and $NbSCl_3$ differ from the experimental ones by only 11−14 cm^{-1}. Further, the values of the bond-stretching internal force constants obtained from theory are very close to those obtained by the "stretching modes only" analysis already mentioned and given in footnotes *b* and *c* to Table 5. For $NbOCl_3$, the theoretical values, in aJ/Å^2, are $f_{(Nb=Y)} = 8.108$, $f_{(Nb-X)} = 2.549$, $f_{(Nb-X,Nb-X)} = 0.136$, and $f_{(Nb=Y,Nb-X)} = 0.230$; and for $NbSCl_3$, they are $f_{(Nb=Y)} = 4.573$, $f_{(Nb-X)} = 1.870$, $f_{(Nb-X,Nb-X)} = -0.542$, and $f_{(Nb=Y,Nb-X)} = 0.166$.

Electron Diffraction. Curves of the total scattered intensities (s^4I_T) for $NbSCl_3$ are shown in Figure 3 along with the background-subtracted molecular intensity curves ($sI_M(s)$), the form used in the least squares refinement procedure.[26] Curves for $NbOBr_3$ and $NbSBr_3$ are similar and can be found in the Supporting Information. With use of theoretical intensity data in the unobserved region $s < 2.00$ Å^{-1}, experimental radial distribution (RD) curves (Figures 4−6)

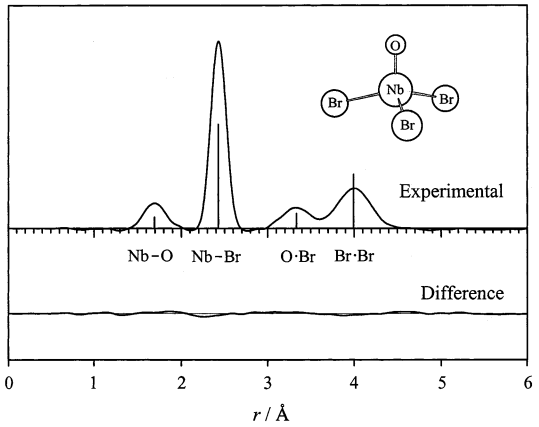

Figure 4. Radial distribution curve for $NbOBr_3$. The vertical bars show the positions and relative weights of the interatomic distances. The difference curves are experimental minus theoretical for the final model (A). See Table 6 for model details.

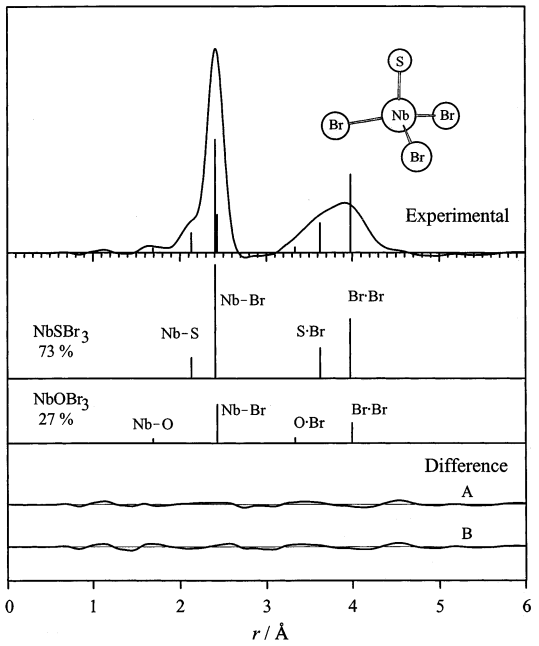

Figure 5. Radial distribution curve for $NbSBr_3$. The difference curves (experimental minus theoretical) are for the preferred model A and for B which contains no impurity; details are found in Table 6. The vertical bars show the positions and relative weights of the interatomic distances for model A.

were calculated from the function $sI_M(s)_{exp}(Z_{Nb}Z_X/A_{Nb}A_X)\exp(-0.002\ s^2)$ (X = Cl or Br) according to procedures previously described.[26] The electron-scattering factors and phases used in these and other calculations were taken from tables.[27]

As previously reported,[6−8] C_{3v} symmetry for the molecules of $NbOF_3$, $NbOCl_3$, and $NbOI_3$ was consistent with the GED data and adopted as an assumption. The peaks of the RD curves from the present study are also consistent with this symmetry, and accordingly, the same assumption about the molecular geometries was made. Preliminary analysis of the $NbOBr_3$ data led to a good fit for essentially pure material

(26) (a) Hedberg, K.; Iwasaki, M. *Acta Crystallogr.* **1964**, *17*, 529. (b) Hedberg, L. *Abstracts*, Fifth Austin Symposium on Gas-Phase Molecular Structure, Austin, TX, March 1974; p 37. (c) Gundersen, G.; Hedberg, K. *J. Chem. Phys.* **1969**, *51*, 2500.

(27) (a) Elastic amplitudes and phases: Ross, A. W.; Fink, M.; Hilderbrandt, R. L. *International Tables for Crystallography*, International Union of Crystallography; Kluwer: Boston; Vol. 4, p 245. (b) Inelastic amplitudes and phases: Cromer, D. T. *J. Chem. Phys.* **1969**, *50*, 4857.

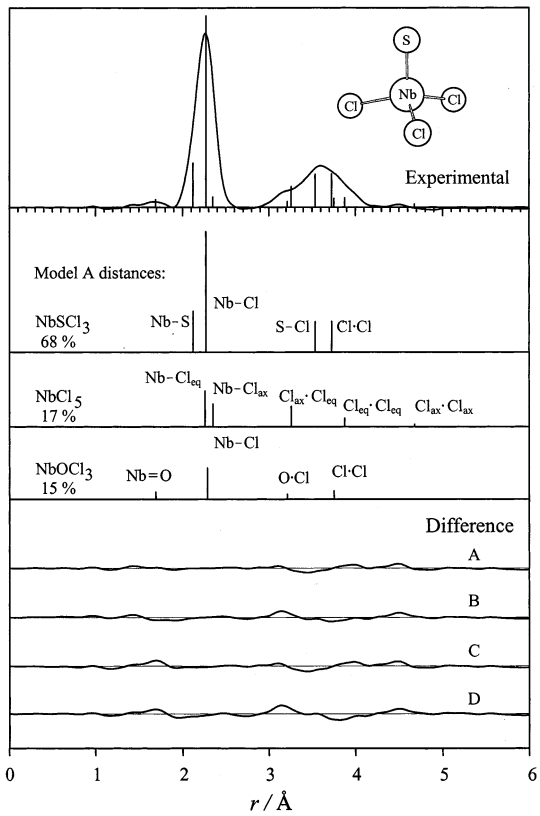

Figure 6. Radial distribution curve for $NbSCl_3$. The difference curves (experimental minus theoretical) A, B, and C are for the models containing possible impurities as described in Table 6. Model D is the result if no impurity is present. The positions of the distances in model A (the preferred model) are shown by the sets of vertical bars with each set weighted according to the amount of each component present.

as the vapor. For $NbSCl_3$ and $NbSBr_3$, however, the preliminary work indicated the presence of sample impurities: each RD curve contains a small peak at about $r = 1.7$ Å, which is shorter than the expected length of an Nb═S bond (2.1 Å), and about equal to the expected length of a Nb═O bond. The likely impurities are thus the oxotrihalides corresponding to $NbOCl_3$ and $NbOBr_3$ because they were found to be present as impurities in the matrix studies of $NbSCl_3$ and $NbSBr_3$. Another impurity concern was the possible presence of $NbCl_5$ in the $NbSCl_3$ sample due to thermal disproportionation during volatilization. The analysis of the $NbSBr_3$ structure thus required allowance for the presence of $NbOBr_3$, and that of $NbSCl_3$ allowance for both $NbOCl_3$ and $NbCl_5$. Fortunately, the structures of each have been determined.[7,22b]

The three structural parameters chosen to define the structures of the $NbYX_3$ molecules were the r_α bond lengths r(Nb═Y) and r(Nb─X), and the bond angle ∠(Y═Nb─X). The r_α distances were converted to the r_a type required by the scattering intensity formula with use of values for centrifugal distortions and perpendicular amplitudes calculated with the program ASYM40 as described in an earlier section. The vibrational parameters were the four rms amplitudes of vibration corresponding to the different types of interatomic distance. The structure refinements were carried out by least squares adjustment of theoretical intensity curves to the experimental ones[26] in the form $sI_m(s)$ using a unit weight matrix.

Table 6. Least-Squares Refinement Results for Various Models of $NbOBr_3$, $NbSBr_3$, and $NbSCl_3$[a,b]

	$NbOBr_3$	$NbSBr_3$[c]		$NbSCl_3$[c]		
param[d]	A	A	B	A	B	C
r(Nb═Y)	1.694(7)	2.134(10)	2.139(10)	2.120(10)	2.131(9)	2.125(10)
r(Nb─X)	2.429(2)	2.408(4)	2.413(3)	2.271(6)	2.278(4)	2.274(6)
r(Y···X)	3.341(11)	3.637(16)	3.636(16)	3.541(29)	3.546(28)	3.544(27)
r(X···X)	4.004(12)	3.986(17)	4.000(14)	3.733(27)	3.752(29)	3.741(25)
l(Nb═Y)	0.044(11)	0.073(10)	0.085(8)	0.036(13)	0.051(10)	0.039(13)
l(Nb─X)	0.062(3)	0.064(3)	0.065(3)	0.055(5)	0.057(5)	0.054(5)
l(Y···X)	0.148(14)	0.167(28)	0.202(31)	0.122(29)	0.164(24)	0.123(30)
l(X···X)	0.192(10)	0.195(21)	0.198(18)	0.154(51)	[0.187]	0.154(50)
∠(Y═Nb─X)	106.9(5)	106.3(7)	105.9(6)	107.4(12)	107.1(13)	107.3(11)
∠(X─Nb─X)	111.0(5)	111.7(6)	112.1(6)	110.5(11)	110.9(12)	110.7(10)
% $NbSX_3$	[0]	73(10)	[100]	68(5)	76(8)	78(8)
% $NbCl_5$[e]	[0]	[0]	[0]	17(5)	[0]	22(8)
% $NbOX_3$[e]	[100]	27(10)	[0]	15(5)	24(9)	[0]
R[f]	0.08	0.10	0.11	0.12	0.13	0.13

[a] C_{3v} symmetry assumed for all models. [b] Distances (r_g) and amplitudes (l) are in angstroms, and angles (∠$_g$) are in degrees; uncertainties are 2σ, and quantities in square brackets were assumed. [c] Models of $NbSBr_3$ and $NbSCl_3$ differ in the impurities included. [d] Y = O or S, X = Br or Cl. [e] Structural parameters were taken from this work ($NbOBr_3$) and refs 22b ($NbCl_5$) and 7 ($NbOCl_3$). [f] Goodness of fit factor: $R = [\sum_i w_i \Delta_i^2 / w_i I_i(\text{obsd})^2]^{1/2}$ with $\Delta_i = I_i(\text{obsd}) - I_i(\text{calcd})$ and $I_i = s_i I_i$.

For $NbOBr_3$ with no evidence of impurity, all structural and vibrational amplitude parameters refined smoothly to the results given in Table 6. The difference curve in Figure 4 shows that the final model provides an excellent fit to the experimental data.

With the details of the $NbOBr_3$ structure available, account could be taken of its presence in the $NbSBr_3$ diffraction data by adding the known values of its interatomic distances and vibrational amplitudes to the model and refining only its amount with use of a mole-fraction parameter. The best fit to the data was obtained with system model A that contained a ratio of $NbSBr_3/NbOBr_3$ of about 3/1. For comparison, refinements were also carried out on a model B in which the $NbOBr_3$ impurity was omitted. The $r_g/\angle_g$ parameter values for both models are found in Table 7. The quality-of-fit factors R for the two models as well as the difference curves of Figure 5 indicate that model A provides somewhat better agreement with experiment than model B.

The analysis of the $NbSCl_3$ system was the most complicated because allowance for the possible presence of two impurities, $NbCl_5$ unreacted from the preparation and $NbOCl_3$ from oxidation of the product, was required. Three models consisting of $NbSCl_3$ and various combinations of the impurities were tested: model A contained both impurities, B had only $NbOCl_3$, and C had only $NbCl_5$. A model D containing no impurity was also tested, but the results have not been tabulated because, as may be seen in Figure 6, it gave much poorer agreement than the others. In preliminary refinements, attempts were made to measure the structures of the impurities together with that of $NbSCl_3$, but the results were poor. Instead, the impurity structures were taken from the literature: $NbCl_5$ with assumed D_{3h} symmetry[22b] and $NbOCl_3$ with C_{3v}.[7] All of the structural and vibrational-amplitude parameters associated with $NbSCl_3$ were refined together with two composition parameters for the supposed

Table 7. Structural and Vibrational Results for Preferred Models of $NbOBr_3$, $NbSBr_3$, and $NbSCl_3$[a]

	experiment[b]				theory, B3LYP/		
	$r_\alpha/\angle_\alpha$	$r_g/\angle_g$	$r_a/\angle_a$	l	Stuttgart[c]	H−W[d]	l[c]
			$NbOBr_3$				
Nb═O	1.682	1.694(7)	1.693	0.044(11)	1.709	1.700	0.039
		1.694	*1.692(8)*	*0.044(11)*			
Nb−Br	2.417	2.429(2)	2.427	0.062(3)	2.451	2.452	0.062
		2.429	*2.427(2)*	*0.062(3)*			
O···Br	3.330	3.341(11)	3.334	0.148(14)	3.384	3.375	0.140
		3.344	*3.337(19)*	*0.148(14)*			
Br···Br	3.996	4.004(12)	3.995	0.192(10)	4.049	4.054	0.198
		4.005	*3.995(12)*	*0.192(10)*			
∠(O═Nb−Br)	107.3(5)		*106.8(9)*		107.5	107.4	
∠(Br−Nb−Br)	111.5(5)		*110.8(9)*		111.4	111.5	
% $NbOBr_3$	[100]		*[100]*				
R[e]	0.079		*0.079*				
			$NbSBr_3$				
Nb═S	2.123	2.134(10)	2.131	0.073(10)	2.144	2.141	0.059
Nb−Br	2.397	2.408(4)	2.406	0.064(3)	2.444	2.444	0.059
S···Br	3.628	3.637(16)	3.629	0.167(28)	3.717	3.711	0.177
Br···Br	3.978	3.986(17)	3.976	0.195(21)	4.025	4.030	0.187
∠(S═Nb−Br)	106.6	106.3(7)	106.1		108.0	107.9	
∠(Br−Nb−Br)	112.2	111.7(6)	111.4		110.9	111.0	
% $NbSBr_3$		73(9)					
% $NbOBr_3$[f]		27(9)					
R[e]		0.097					
			$NbSCl_3$				
Nb═S	2.112	2.120(10)	2.120	0.036(13)	2.143	2.142	0.046
Nb−Cl	2.259	2.271(6)	2.270	0.055(5)	2.296	2.295	0.058
S···Cl	3.533	3.541(29)	3.537	0.122(29)	3.590	3.588	0.145
Cl···Cl	3.725	3.733(27)	3.726	0.154(51)	3.782	3.784	0.187
∠(S═Nb−Cl)	107.8	107.4(12)	107.3		107.9	107.9	
∠(Cl−Nb−Cl)	111.1	110.5(11)	110.4		111.0	111.0	
% $NbSCl_3$		68(5)					
% $NbCl_5$[g]		17(5)					
% $NbOCl_3$[g]		15(5)					
R[e]		0.123					

[a] Preferred models are A of Table 4. Distances (r) and amplitudes (l) in angstroms, angles (∠) in degrees. Uncertainties are 2σ. [b] Symmetry C_{3v} assumed except for items in italics which result from refinements of all distances unrestricted by symmetry. [c] Basis sets were Stuttgart RSC ECP for Nb and 6-311G* for O, S, Cl, and Br. [d] Basis sets were Hay−Wadt VDZ ($n + 1$) ECP for Nb and aug-cc-pVTZ for O, S, Cl, and Br. [e] Goodness of fit factor: See footnotes to Table 4. [f] Structural parameters for the impurity $NbOBr_3$ are given in this table. [g] Structural parameters for impurities $NbCl_5$ ($\langle r_\alpha(Nb{-}Cl)\rangle = 2.280$ and $\Delta\gamma_\alpha(Nb{-}Cl_{ax} - Nb{-}Cl_{eq}) = 0.097$) and $NbOCl_3$ ($r_\alpha(Nb{=}O) = 1.682$, $r_\alpha(Nb{-}Cl) = 2.276$, and $\angle(O{=}Nb{-}Cl) = 107.5$) were taken from refs 22b and 7, respectively.

impurities. The parameter values for all models are given in Table 6. It can be seen from the R values that model A produces the best fit to experiment, a conclusion supported by the difference curves in Figure 6. Table 7 contains the experimental structural and vibrational details of the preferred models (A) for each of the compounds, together with theoretical values. Also found in the table are results for an independent distance model of $NbOBr_3$ that will be discussed later, and the parameters of the structures of the three $NbYX_3$ molecules predicted by theory. Table 8 contains the correlation matrices.

Discussion

It has been found that theoretical values for single-bond lengths at the HF level of theory often compare well with experimental (r_a) ones when an offset value of ~0.02 Å has been applied to the former. It is uncertain whether use of the offset value is appropriate for the higher levels of theory used for the molecules of Table 7, but it is worth pointing out that this correction brings all the theoretical bond lengths quite close to those observed. In any case, the theoretical bond angles are in excellent agreement with observation with differences of only 1.0−1.5°.

Of the three molecules studied in this investigation, only $NbOBr_3$ has the four interatomic distances sufficiently resolved in the radial distribution curve to allow their simultaneous, individual, refinement independent of the structural constraints imposed by the C_{3v} symmetry of the molecule. The values from such a refinement differ in principle from those obtained by a symmetry-constrained refinement due to the effects of vibrational averaging ("shrinkage"); however, the effects for our $NbYX_3$ molecules are expected to be very small because the vibrational amplitudes are themselves small. The results from refinement of all distances as independent variables for $NbOBr_3$ are the italicized values listed as r_a in Table 7 (the r_g ones are calculated from them). The magnitude of the "experimental shrinkage" for $NbOBr_3$ may be expressed in different ways, but the following is perhaps the simplest. Use of the C_{3v}-consistent values 107.3° for the bond angle O═Nb−Br and 111.5° for Br−Nb−Br together with the r_a bond lengths from the independent-distance refinement (values in italics) leads to predicted O···Br and Br···Br distances of 3.347(14) and 4.014(8) Å. The measured (independent-distance) values at 3.337(9) and 3.995(6) Å[28] are shorter than these by about 0.010 and 0.019 Å, respectively; these are the experimental

Table 8. Correlation Matrices (×100) and Standard Deviations for Parameters of the Preferred Models of the $NbYX_3$ Molecules[a]

param	σ_{LS}[b]	r_1	r_2	$\angle_3$	l_4	l_5	l_6	l_7	χ_8
				$NbOBr_3$					
1 r(Nb−O)	0.25	100							
2 r(Nb−Br)	0.02	−4	100						
3 ∠(O−Nb−Br)	18	−15	10	100					
4 l(Nb−O)	0.39	−5	−3	1	100				
5 l(Nb−Br)	0.02	−1	1	9	2	100			
6 l(O···Br)	0.45	2	−2	−7	−2	3	100		
7 l(Br···Br)	0.24	−3	−1	3	3	12	−30	100	
				$NbSBr_3$					
1 r(Nb−S)	0.33	100							
2 r(Nb−Br)	0.10	16	100						
3 ∠(S−Nb−Br)	25	−28	−27	100					
4 l(Nb−S)	0.33	10	63	−17	100				
5 l(Nb−Br)	0.05	12	20	−12	−2	100			
6 l(S···Br)	0.94	11	48	−21	31	18	100		
7 l(Br···Br)	0.67	2	3	−5	1	8	57	100	
8 χ[c]	3.3	19	94	−30	60	30	52	4	100
				$NbSCl_3$					
1 r(Nb−S)	0.34	100							
2 r(Nb−Cl)	0.22	86	100						
3 ∠(S−Nb−Cl)	42	−6	−3	100					
4 l(Nb−S)	0.46	32	53	3	100				
5 l(Nb−Cl)	0.15	−26	−5	3	64	100			
6 l(S···Cl)	1.0	38	50	62	43	12	100		
7 l(Cl···Cl)	1.8	35	44	72	34	7	87	100	
8 χ[c]	1.8	72	90	2	68	10	59	50	100

[a] Distances (r) and amplitudes (l) in angstroms, angles (∠) in degrees. [b] Standard deviations ×100 from least-squares fitting. [c] Mole fraction.

r_a shrinkages in the nonbond distances. Slightly different values are found for the r_g shrinkages: 0.005 and 0.012 Å. Shrinkages may also be obtained solely from the C_{3v}-consistent results by similar calculations. For example, use of the r_a values (regular typeface) for the bonds and the r_α bond angles yields 0.013 and 0.019 Å for the respective shrinkages of the O···Br and Br···Br distances. Although the significance of these differences can be debated, the various sets of shrinkage values are consistent with the expected small amount of shrinkage in the $NbYX_3$ molecules. It is also evidence for the accuracy of the correction factors for distances that play an important role in refinements based on symmetry-consistent r_α space.

A comparison of the structural results obtained from the present work with those previously reported for other chalcogenide trihalides ($NbOF_3$,[6] $NbOCl_3$,[7] and $NbOI_3$[8]) is presented in Table 9. All models assume molecules of C_{3v} symmetry. An interesting feature of Table 9 is the near constancy of the bond lengths of a given type. Thus, the four Nb═O distances differ at most by only 0.014 Å, and if $NbOI_3$ is excluded, by only 0.001 Å, and the values themselves lie well within the range 1.66−1.71 Å observed for a broad range of niobium−oxygen terminal bonds.[29] Likewise, the pairs of Nb═S, Nb−Cl, and Nb−Br distances differ, respectively, by only 0.011, 0.018, and 0.021 Å. One may conclude that in these molecules the nature of the bonding to a given ligand is not much affected by the nature of the other ligands. Another interesting feature of Table 9 is the near constancy of the values of the two angle parameters ∠Y═Nb−X and ∠X−Nb−X, which deviate no more than 0.8° from their respective averages of 106.8° and 110.6°. This angle constancy seems surprising because of the large size difference of the ligands. However, a similar phenomenon was observed for the C_{4v} symmetry tungsten chalcogenide tetrahalide molecules WYX_4 (Y = O, S, or Se; X = F, Cl, Br) and was explained as the consequence of a balancing of electrostatic and steric forces between the ligands.[4] We have investigated the possibility that a similar balancing also occurs in the niobium compounds. Table 10 lists estimates, relative to each other within each type, of the electrostatic and steric forces between the ligands in several niobium compounds. One sees immediately that steric effects cannot play an important role in most of these compounds because the van der Waals distances X···Y and X···X are generally less than the experimental ones. The possible exceptions are the X···Y type repulsions in $NbSCl_3$ and $NbSBr_3$; however, the van der Waals radii used in the calculations are doubtless too large for atoms at the ends of adjacent bonds, so that it is reasonable to expect all measured nonbond distances to be greater than the sum of the van der Waals radii. The constancy of the bond angles thus seems to depend on differences in the electrostatic repulsions

Table 9. Distances (r_a/Å), Amplitudes (l/Å), and Bond Angles ($\angle_a$/deg) for $NbYX_3$ Molecules from Gas-Phase Electron Diffraction[a]

param	$NbOF_3$	$NbOCl_3$	$NbOBr_3$	$NbOI_3$	$NbSCl_3$	$NbSBr_3$
r(N═Y)	1.694(5)	1.693(4)	1.693(7)	1.717(3)	2.120(10)	2.131(10)
r(Nb−X)	1.871(1)	2.288(1)	2.427(2)	2.652(2)	2.270(6)	2.406(4)
r(Y···X)	2.858(18)	3.218(7)	3.334(11)	3.564(3)	3.537(29)	3.629(16)
r(X···X)	3.076(17)	3.752(8)	3.995(12)	4.345(2)	3.726(27)	3.976(17)
l(N═Y)	0.043(3)	0.045(6)	0.044(11)	0.092(3)	0.036(13)	0.073(10)
l(Nb−X)	0.051(3)	0.066(1)	0.062(3)	0.075(2)	0.055(5)	0.064(3)
l(Y···X)	0.133(20)	0.146(10)	0.148(14)	0.140(3)	0.122(29)	0.167(28)
l(X···X)	0.155(20)	0.217(11)	0.192(10)	0.249(1)	0.154(51)	0.195(21)
∠Y═Nb−X[b]	106.5(1)	106.9(0.4)	106.7(5)	107.4	107.3(12)	106.1(7)
∠X−Nb−X[b]	110.6	110.2	110.7(5)	110.0	110.4(11)	111.4(6)
temp/K	864	743	600	698	582	541
% impurity	2(2)[c]			21[d]	17(5)[e]	25(10)[f]
				4[g]	15(5)[h]	
ref	6	7	this work	8	this work	this work

[a] Values in parentheses are 2σ. [b] Calculated from r_a distances. [c] NbF_5. [d] NbI_4. [e] $NbCl_5$. [f] $NbOBr_3$. [g] I_2. [h] $NbOCl_3$.

Table 10. Electrostatic and Steric Effects in Niobium Chalcogen Halides

	$NbOF_3$	$NbOCl_3$	$NbOBr_3$	$NbOI_3$	$NbSCl_3$	$NbSBr_3$
			Mulliken charges[a]			
Y	−0.46	−0.40	−0.41	−0.41	−0.19	−0.21
X	−0.43	−0.30	−0.19	−0.11	−0.29	−0.17
			electrostatic effects[b]			
X···Y	2.4	1.6	0.7	0.4	0.4	0.3
X···X	1.9	1.2	0.2	0.1	0.6	0.2
			van der Waals radii[c]			
Y	1.40	1.40	1.40	1.40	1.85	1.85
X	1.35	1.80	1.95	2.15	1.80	1.95
			steric effects[d]			
X···Y	0.11	0.02	−0.02	0.01	−0.11	−0.17
X···X	0.38	0.15	0.10	0.04	0.13	0.08

[a] From the B3LYP/Stuttgart theoretical results; see Table 4. [b] Relative repulsion forces equal to $100Q_iQ_j/r^2_{exp}$. [c] Taken from: Pauling, L. *The Nature of the Chemical Bond*, 3rd Ed.; Cornell University Press: Ithaca, NY, 1960; p 260. [d] Relative repulsion forces equal to $r_a - d_{vdW}$.

(28) The uncertainties given here differ from those in Table 7 by the terms representing possible wavelength error present in the latter. For comparison with each other, any wavelength error would be canceled out.

(29) See: Drew, M. G. B.; Rice, D. A.; Williams, D. M. *Inorg. Chim. Acta* **1986**, *118*, 165 and references contained therein.

between the X···Y and X···X atomic pairs, a simpler situation than in the tungsten compounds where both electrostatic and steric effects had to be invoked to account for the angles. These differences are seen to be similar (X···Y slightly greater than X···X) throughout the series of molecules, with the sole exception of $NbSCl_3$ where X···X is slightly larger. We conclude that the bond angles in these niobium compounds are consistent with electrostatic and steric effects that might be expected to play a role in determining their values.

Acknowledgment. This work was supported by the National Science Foundation under Grant CHE99-87359 and NATO under Grant CRG 910203. We are grateful to the EU for award of a grant to I.N.

Supporting Information Available: Tables of averaged molecular intensities, and figures of the intensity curves, for $NbOBr_3$ and $NbSBr_3$. This material is available free of charge via the Internet at http://pubs.acs.org.

IC020405F